Effects of vacancies in the triangular spin-$\frac{1}{2}$ antiferromagnet

C. L. O'Donnell and David Y. K. Ko
Theoretical Physics, University of Oxford, 1 Keble Road, Oxford OX1 3NP, England
(Received 21 March 1994)

We examine the effects of vacancies on a triangular spin-$\frac{1}{2}$ antiferromagnet within spin-wave theory. We find that frustration is dominant in determining the properties of the defective lattice. For a single vacancy the on-site magnetization is significantly modified over a large region. For more than one vacancy the change in the magnetization is found to depend on their relative positions and not simply on their distance of separation. The qualitative behavior may be understood in terms of the relief of frustration. We also consider *kagomé* patches of various sizes embedded in an infinite triangular lattice, and find that the change in the density of states leads to a low-temperature peak in the specific heat.

Defects in localized magnetic systems have long been a subject of interest. Early studies by Lovesey,[1,2] Wolfram and Calloway,[3] Walker *et al.*[4] and others have concentrated on the problem in three-dimensional ferromagnetic and antiferromagnetic systems and more recently, Chen and Cottam[5] and others have examined the presence of defect states on crystal surfaces. Similar studies of two-dimensional quantum magnets have been motivated by the discovery of strong antiferromagnetic fluctuations in the high-temperature superconductors and by the desire to understand how an antiferromagnetic ground state in two dimensions may be modified by the presence of defects. Work has been carried out by applying spin-wave theory to the Heisenberg antiferromagnet on the square lattice, which has a well-defined sublattice magnetization.[6-8] Bulut *et al.*[9] have shown that a highly localized magnetic polaron state exists around a single vacancy, and for a finite defect density the magnetic order is found to be destroyed.[10] Tanaka and Watanbe[11] have further found in a recent study that even for the case of a line of broken bonds, the effect is still strongly localized to the defect region.

The triangular spin-$\frac{1}{2}$ antiferromagnet is, however, frustrated. Results by Jolicoeur and Le Guillou[12] using spin-wave analysis, by Huse and Elser[13] using a variational calculation, by Nishimori and Nakanashi[14] using numerical diagonalizations, and by Singh and Huse[15] using series expansions have led to the general consensus that the ground state exhibits a finite on-site magnetization, but its value is substantially reduced from $\frac{1}{2}$ and the system is on the verge of disorder. The effect of defects may therefore be stronger than for the square lattice, and it is interesting to examine to what extent the local magnetic ordering is modified depending on the configurations of defects present.

In this paper we present a spin-wave analysis of the effects of vacancies in a two-dimensional triangular spin-$\frac{1}{2}$ antiferromagnet. In the first instance we examined the case of a single vacancy in a triangular lattice, where we find a reduction of the magnetization, the size of which is an order of magnitude greater than that observed for the case of the square lattice, and which extends over a much longer range. The case of several vacancies is also studied, and we see a rapid breakdown in the local order. The breakdown is found to be strongly dependent on the relative positions of the vacancies. The particular arrangement of vacancies in the form of a *kagomé* patch was also considered, and an estimate of the specific heat due to the changes in the local ordering was obtained. This may have some relevance to the problem of ^{3}He on graphite.

The starting point of our analysis is the classical Néel state for a triangular antiferromagnet, where the spins are all coplanar and form three sublattices, each with spin oriented at an angle of $2\pi/3$ to its neighbors. The Hamiltonian is given by

$$H_0=\frac{1}{2}J\sum_{\langle i,j\rangle}\mathbf{S}_i\cdot\mathbf{S}_j\ , \tag{1}$$

with $\langle i,j\rangle$ denoting summation over nearest neighbors only. Vacancies are introduced via the potential

$$V=-\frac{1}{2}J\sum_k\sum_{\langle i,k\rangle}\mathbf{S}_i\cdot\mathbf{S}_k\ , \tag{2}$$

where the summation over k is over the sites containing the vacancies. The potential V thus effectively subtracts out the bonds which connect spins to vacancies. The spin which remains at the vacancy site is thus decoupled from the lattice. The spectral weight of the remaining lattice can be calculated independently of the contribution from the decoupled spin which is a δ function at zero frequency. We shall be concerned solely with the former quantity.

Within linear spin-wave theory for the triangular spin-$\frac{1}{2}$ antiferromagnet,[12,16] the spin operators corresponding to the three sublattices are transformed into boson operators using a Holstein-Primakof transformation[17] and gives, to $O(1/S^2)$, $S_A^x=(\sqrt{2S}/2)(a+a^\dagger)$, $S_A^y=(\sqrt{2S}/2i)(a-a^\dagger)$, $S_A^z=S-a^\dagger a$ for sublattice A; $S_B^x=-(\sqrt{2S}/4)(b+b^\dagger)+(\sqrt{3}/2)(S-b^\dagger b)$, $S_B^y=(\sqrt{2S}/2i)(b-b^\dagger)$, $S_B^z=(\sqrt{3}/2)(\sqrt{2S}/2)(b+b^\dagger)-(1/2)(S-b^\dagger b)$ for sublattice B; and $S_C^x=-(\sqrt{2S}/4)(c+c^\dagger)-(\sqrt{3}/2)(S-c^\dagger c)$, $S_C^y=(\sqrt{2S}/2i)(c-c^\dagger)$, $S_C^z=(\sqrt{3}/2)(\sqrt{2S}/2)(c+c^\dagger)-(1/2)(S-c^\dagger c)$ for sublattice C. In deriving the form of the transformed operators, a rotation of the B and C sublattices by $2\pi/3$ and $4\pi/3$ has been used. The Hamiltonian, to quadratic order in the boson operators, becomes

$$H_0=\frac{J}{2}\left\{\sum_{\langle l,m\rangle}[2(a_l^\dagger a_l+b_m^\dagger b_m)+a_l b_m^\dagger+a_l^\dagger b_m-3(a_l b_m+a_l^\dagger b_m^\dagger)]\right.$$
$$+\sum_{\langle m,n\rangle}[2(b_m^\dagger b_m+c_n^\dagger c_n)+b_m c_n^\dagger+b_m^\dagger c_n-3(b_m c_n+b_m^\dagger c_n^\dagger)]$$
$$\left.+\sum_{\langle n,l\rangle}[2(c_n^\dagger c_n+a_l^\dagger a_l)+c_n a_l^\dagger+c_n^\dagger a_l-3(c_n a_l+c_n^\dagger a_l^\dagger)]\right\}, \tag{3}$$

where l, m, and n signify sites on the A, B, and C sublattices, respectively. The potential due to the vacancies can be similarly transformed.

To obtain the spin-spin correlation functions and the on-site magnetization, we use a Green's-function approach. Green's functions are defined in the following manner:

$$G_{i,j}^{\alpha,\beta}(t)\equiv -i\langle T[\alpha_i(t),\beta_j^\dagger(0)]\rangle ,$$
$$F_{i,j}^{\alpha,\beta}(t)\equiv -i\langle T[\alpha_i^\dagger(t),\beta_j^\dagger(0)]\rangle , \tag{4}$$

with α,β being the boson operators corresponding to one of the three sublattices. Given the relation between the spin operators and the Holstein-Primakoff bosons, the spin-spin correlation functions can be readily expressed in terms of the Green's functions. The equation of motion for the Green's functions can be obtained in the usual manner.[1,18] After Fourier transforming in time, the resulting Dyson equation for the case with vacancies may be solved exactly by the matrix inversion

$$\mathbf{G}=\mathbf{G}_0(1+\mathbf{G}_0\mathbf{V})^{-1} . \tag{5}$$

The Green's-function matrix is given by

$$\mathbf{G}=\begin{bmatrix} G_{i,j}(\omega) & F_{i,j}(\omega) \\ F_{i,j}(\omega) & G_{i,j}(-\omega)\end{bmatrix},$$

where i,j are site labels of the lattice, and $\mathbf{G}_0=\mathbf{H}_0^{-1}$ is the Green's function for the perfect triangular lattice.[12] Where possible, the point-group symmetry of the lattice is used to aid in the calculation of the full Green's function.[1,9,19] The clusters we consider contain 271 sites in total, and correspond to nine shells of spins around a central site.

We consider first the case of a single vacancy. The configuration is given in Fig. 1. Because of the inherent symmetry in the lattice, only a twelfth of the cluster is used to present the results. The on-site magnetization, $\langle S^z\rangle_{\text{imp}}$, for the spins which are nearest neighbors of the vacancy is found to be $\langle S^z\rangle=0.160$. This is to be compared with the value $\langle S^z\rangle_0=0.24$ obtained from our calculations for the perfect lattice, in agreement with the spin-wave result of Jolicoeur and Le Guillou,[12] and represents a 32.5% *decrease* below the pure value. The values for the on-site magnetization for the spins further away from the vacancy is shown in Fig. 2. We find that even at a distance of nine shells away from the vacancy, the on site magnetization is still noticeably modified. Thus, the magnetic ordering in the triangular system is strongly suppressed by the presence of even a single defect. The fact that the magnetization next to the vacancy is reduced in contrast to the square lattice case[9] may be due to the fact that the spins are still frustrated and this frustration prevents them from ordering. Consequently the quantum fluctuations play a relatively more important role. Overall, the total deviation $\sum_i\langle S_i^z\rangle-\langle S^z\rangle_0\sim -0.5$.

Figure 3 shows the values obtained for the bond energies

$$\epsilon_{ij}=\tfrac{1}{2}\langle \mathbf{S}_i\cdot\mathbf{S}_j\rangle , \tag{6}$$

where i and j are nearest neighbors. The results show that bonds become less stable where the on-site magnetization is reduced. The long-ranged nature of the effect of introducing a vacancy to the triangular lattice is immediately apparent from the fact that 13 shells of spins must be taken into account before the pure lattice bond energies are resumed. The energy cost of introducing a vacancy to the triangular lattice is 1.074J. Since the cost of breaking six bonds is 1.128J, this implies that the remaining spins are able to adjust their correlations with their

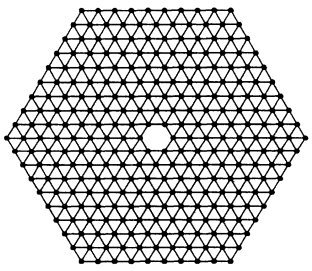

FIG. 1. A cluster of 270 spins in a triangular lattice with a single vacancy.

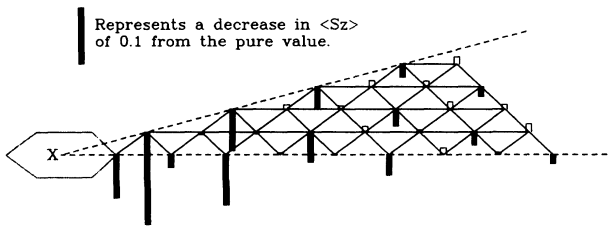

FIG. 2. Schematic diagram showing the change in $\langle S^z\rangle$ due to the introduction of a vacancy for one-twelfth of the cluster. The full cluster can be generated by repeated reflection about the dashed lines. The black columns represent a decrease in $\langle S^z\rangle$; the white columns, an increase. The label X marks the site of the vacancy.

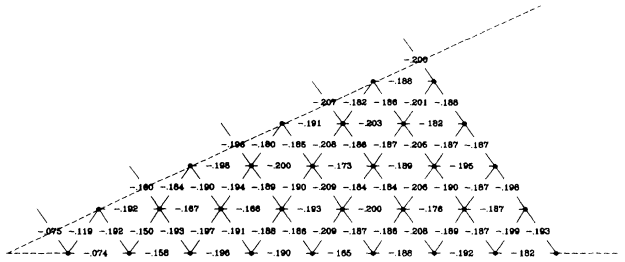

FIG. 3. Bond energies throughout one-twelfth of the cluster. The entire cluster is generated through repeated reflections across the dashed lines.

neighbors to lower the energy of the system.

Figure 4 shows a graph of the change in the density of states, which may be obtained from,[18]

$$\Delta\rho=\rho-\rho^0$$
$$=-\frac{1}{\pi}\mathrm{Im}\left[\frac{d}{d\omega}\ln\{\det[1-(\omega+i\eta-H_0)^{-1}V]\}\right]. \quad (7)$$

$i\eta$ is an imaginary infinitesimal. The figure shows a reduction in the density of states at $\omega\sim0.24$, a resonance at $\omega=\frac{2}{3}$, and a reduction at the band edge. The contributions from the different symmetry components of the vacancy modes can be resolved to show that the first dip is entirely due to s-like modes, whilst the resonance at $\omega=\frac{2}{3}$ occurs because of f-like modes. The resonance at $\omega=\frac{2}{3}$ corresponds to the logarithmic van Hove singularity in the perfect lattice density of states which arises as a result of a saddle point in the energy dispersion.

The effect of introducing a second vacancy to the triangular lattice has also been examined. The results are found to depend very strongly on the actual position of the second vacancy relative to the first and not simply on the absolute distance between them. This is related to the frustrated nature of the lattice. Because of the breaking of the sixfold symmetry of the lattice, the solution of the real-space Dyson equation is more complicated and we

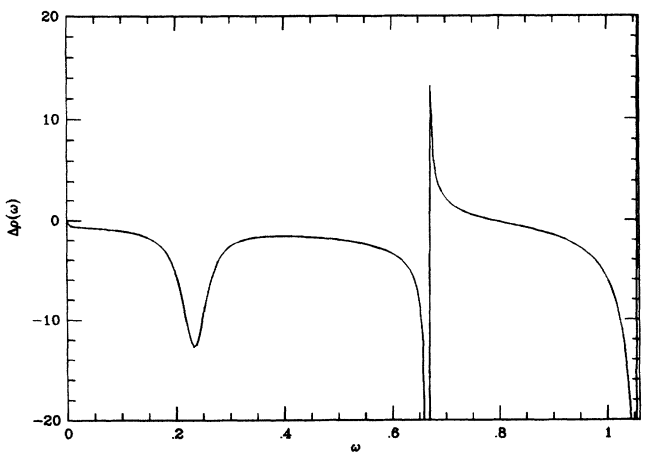

FIG. 4. Graph showing the change in the density of states on the removal of a single spin.

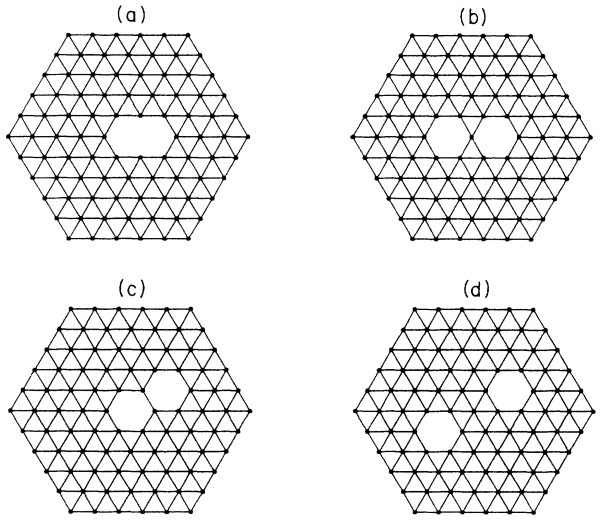

FIG. 5. Schematic diagrams showing the systems of two vacancies studied. (a) and (b) have vacancies in the (1,0) direction, (c) and (d) have vacancies in the $(1,\sqrt{3}/3)$ direction.

considered 91 site clusters. The configurations are shown in Fig. 5. Figures 5(a) and 5(b) correspond to vacancies along the (1,0) direction, with the vacancies being nearest neighbors in (a) and separated by a distance of $2a$ in (b). a is the lattice parameter. For Figs. 5(c) and 5(d), the vacancies are along the $(1,1/\sqrt{3})$ direction, and are separated by $\sqrt{3}a$ and $2\sqrt{3}a$, respectively.

The on-site magnetization for the configurations considered are shown in Fig. 6. For the case of 6(a) where the two vacancies are nearest neighbors, we find that the reduction in the on-site magnetization is less than that obtained for the single vacancy, and that the effect ap-

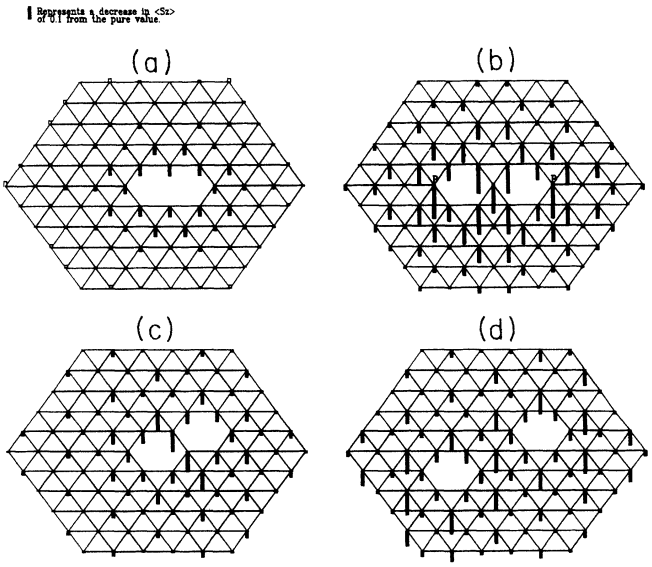

FIG. 6. Schematic diagram showing the change in $\langle S^z\rangle$ due to the introduction of two vacancies in the (1,0) direction, (a) and (b); and in the $(1,\sqrt{3}/3)$ direction, (c) and (d). The black columns represent a decrease in $\langle S^z\rangle$; the white columns, an increase. The label X marks the site of the vacancy, P indicates that the magnetization has a divergent value.

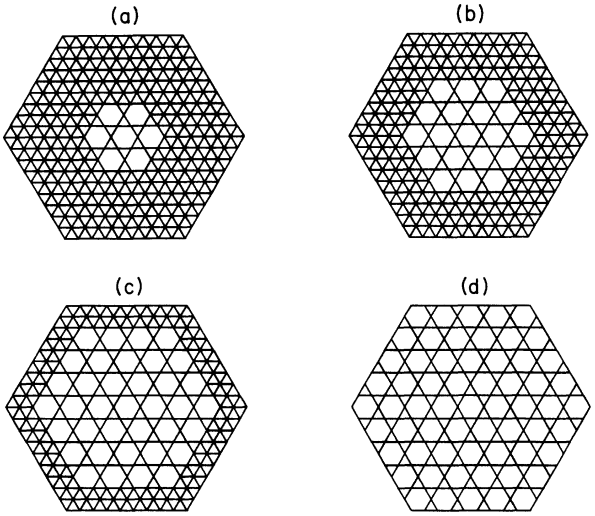

FIG. 7. Clusters of increasing size of *kagomé* patch.

pears to be much shorter ranged. There thus appears to be some cancellation effect from the second vacancy. This is also reflected to some extent in configuration 6(c) where the line connecting the two vacancies bisect a single bond. In contrast, the results of 6(b) and 6(d), where the line connecting the two vacancies cuts through sites still occupied by spins show a marked suppression of the on-site magnetization for sites near the vacancies, with significant deviations from the perfect lattice value found throughout the entire cluster . The pattern of behavior in the on-site magnetization for the different configurations can be understood by considering the frustration remaining in the system. For a system with stronger frustration, the on-site magnetization will be smaller. Since the degree of frustration increases with the number of frustrated triangles of spins, the greater the number of frustrated triangles of spins connected to the defect region, the greater the reduction in the on-site magnetization. A simple counting shows that for the configurations (a), (c), (b), and (d) this number is 30, 36, 42, and 48, respectively, in agreement with the trend observed.

The results for the bond energies (Table I) show that in general, ϵ_{ij} is higher for bonds in the vicinity of the vacancies and slowly decrease to the bulk value away from the vacancies. The bond energies for some of the bonds near the vacancies are shown in Table I, and we find that configuration (b) with the vacancies lying in the (1,0) direction separated by a single spin has the lowest overall energy. For this configuration, an estimate of the total energy of the cluster indicates that the $E(2)-E(1)\sim 0.03J$, where $E(n)$ is the energy the cluster with n vacancies. This is much smaller than the energy cost of introducing one vacancy $E(1)-E(0)\sim 1.1J$, and suggests that the cost of introducing vacancies is marginal in this configuration. For the other configurations the cost of introducing the second vacancy is significantly higher.

We have also considered the case of vacancies arranged in the form of *kagomé* patches embedded in an infinite triangular lattice. The configurations examined are shown in Fig. 7. The infinite *kagomé* lattice has been discussed

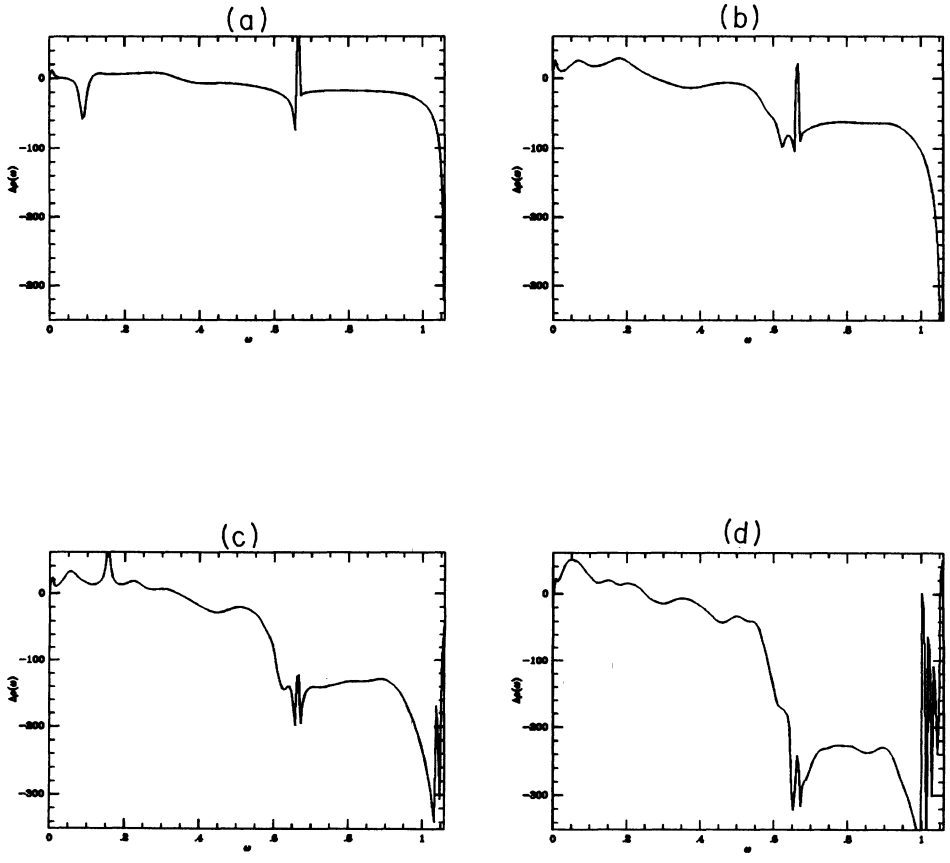

FIG. 8. Graphs showing the change in the density of states from the triangular lattice values as the size of the patch increases. (a)–(d) correspond to patches containing 1–4 *kagomé* layers, respectively.

TABLE I. Bond energies for a system with two vacancies in the (1,0) direction, (a) and (b); and in the $(1,\sqrt{3}/3)$ direction, (c) and (d).

Distance of midpoint of bond from central spin in lattice spacings	Bond Energies (J) (a)	(b)	(c)	(d)
1				−0.114
2			−0.011	−0.065
3	−0.101	−0.135	−0.141	−0.139
4	−0.159	−0.108	−0.196	−0.202
5	−0.167	−0.208	−0.180	−0.190
$\sqrt{3}/2$			−0.011	−0.077
$3\sqrt{3}/2$	−0.188	−0.202	−0.033	−0.051
$5\sqrt{3}/2$	−0.195	−0.238	−0.180	−0.169

by various authors.[20–28] Due to the presence of the so-called "weather-vane" modes associated with the uniform rotation of all six spins in a hexagon surrounding a vacant site, the classical ground sate is infinitely degenerate and hence disordered. The energy of the weather-vane modes is zero for all k values.[21] The quantum ground state is also believed to be disordered.[20,23] However, suggestions of order from disorder behavior due to quantum fluctuations exist.[27] Studies of ^{3}He deposited on graphite[29,30] indicate that for partial coverage of the second monolayer a *kagomé* configuration of the He atoms may be formed, with the nuclear moment of the He atoms acting as a spin-$\frac{1}{2}$ antiferromagnet. Our results for the two vacancy configurations suggest that the *kagomé*-like system has a low energy. We note that we cannot describe the weather-vane modes, and so our results are essentially restricted to the fluctuations due to the normal excitations.

Analysis of the contribution to the on-site magnetization reduction from the normal excitations show that for the configurations (b), (c), and (d) shown in Fig. 7 the on-site magnetization for spins near the vacancies become divergent. This is associated with the breakdown of spin-wave theory and clearly suggests the breakdown of the antiferromagnetic order even without the weather-vane modes. The change in the density of states, shown in Fig. 8, indicates a gradual buildup at low energies with increasing patch size. From the change in the density of states, the change in the heat capacity may also be obtained. Since for a spin-$\frac{1}{2}$ system the number of spin excitations per site is restricted to no more than one, it is more appropriate to use a Fermi-Dirac distribution to describe the occupation of the excitations. This is essentially to reimpose the boson occupation number constraint which was relaxed in the first-order expansion of the Holstein-Primakoff transformation. The results for the different patch sizes are shown in Fig. 9 and demonstrate, as shown in the inset, a very low-energy peak associated with the shifting of the density of states. The temperature of the peak corresponds to $T\sim 0.3$ mK, and is of the order of that experimentally predicted for ^{3}He and corresponds well with other theoretical estimates.[23,28]

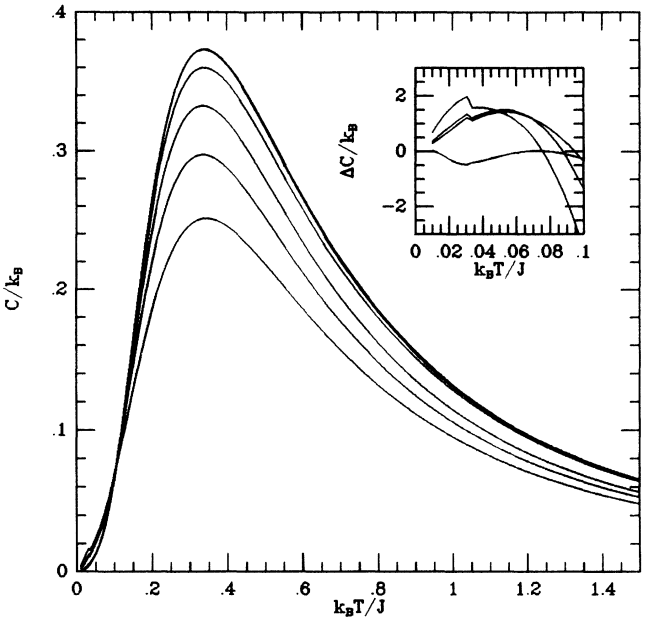

FIG. 9. The specific heat per spin in the cluster in units of k_B versus temperature in units of J/k_B. The uppermost curves are the heat capacities of the perfect triangular lattice and with one spin removed. The inset shows the change in the heat capacity at low temperatures.

We have presented an analysis of the effects of vacancies on a triangular spin-$\frac{1}{2}$ antiferromagnet. The results show that frustration remains the dominant influence even in the presence of defects, leading to longer range effects than were observed for a square lattice. The reduction in the magnetization for two vacancies was found to be related to the reduction in the frustration, and not directly associated with the distance between the vacancies. For the *kagomé* system we find that even without the weather-wave modes the antiferromagnetic order is rapidly destroyed. We have attempted to analyze the heat-capacity changes associated with the buildup of *kagomé* symmetry related states and find a peak at low temperature which is in qualitative agreement with experimental predictions.

LO'D acknowledges stimulating discussions with H. U. Everts and thanks the Institut für Theoretische Physik at the Universität Hannover for its hospitality during the visit when this work was initiated. Partial support for the visit was provided by ERASMUS, St. Hilda's College, Oxford and the Universität Hannover. LO'D also acknowledges financial support from the Department of Education for Northern Ireland and DYKK Grant No. GR/H26680 of the SERC of U.K.

[1]S. W. Lovesey, J. Phys. C **1**, 102 (1968).
[2]S. W. Lovesey, J. Phys. C **1**, 118 (1968).
[3]T. Wolfram and J. Calloway, Phys. Rev. **130**, 2207 (1963).
[4]L. R. Walker, C. B. Chambers, D. Hone, and Herbert Callan, Phys. Rev. B **5**, 1144 (1972).
[5]N. N. Chen and M. J. Cottam, Phys. Rev. B **45**, 266 (1992).
[6]M. Parrinello and T. Arau, Phys. Rev. B **10**, 265 (1974).
[7]J. Oitma and D. D. Betts, Can. J. Phys. **56**, 897 (1978).
[8]M. Gross, E. Sanchez-Velasco, and E. Siggia, Phys. Rev. B **39**, 2484 (1989).
[9]N. Bulut, D. Hone, D. J. Scalapino, and E. Y. Loh, Phys. Rev. Lett. **62**, 2192 (1989).
[10]D. Y. K. Ko, Phys. Rev. Lett. **65**, 116 (1990).
[11]Y. Tanaka and K. Watanbe, J. Phys. Soc. Jpn. **62**, 4531 (1993).
[12]Th. Jolicoeur and J. C. Le Guillou, Phys. Rev. B **40**, 2727 (1989).
[13]D. A. Huse and V. Elser, Phys. Rev. Lett. **60**, 2531 (1988).
[14]H. Nishimori and N. Nakanashi, J. Phys. Soc. Jpn. **57**, 626 (1988).
[15]R. R. P. Singh and D. A. Huse, Phys. Rev. Lett. **68**, 1766 (1992).
[16]Tosizumi Aoki, J. Phys. Soc. Jpn. **62**, 2462 (1993).
[17]T. Holstein and H. Primakoff, Phys. Rev. **58**, 1098 (1940).
[18]D. N. Zubarev, Sov. Phys. Usp. **3**, 320 (1960).
[19]J. P. Elliott and P. G. Dawber, *Symmetry in Physics* (Macmillan Education, London, 1979).
[20]J. T. Chalker, P. C. B. Holdsworth, and E. F. Shender, Phys. Rev. Lett. **68**, 855 (1992).
[21]A. B. Harris, C. Kallin, and A. J. Berlinsky, Phys. Rev. B **45**, 2899 (1992).
[22]C. Zeng and V. Elser, Phys. Rev. B **42**, 8436 (1990).
[23]V. Elser, Phys. Rev. Lett. **62**, 2405 (1989).
[24]S. Sachdev, Phys. Rev. B **45**, 12 377 (1992).
[25]J. T. Chalker and J. F. G. Eastmond, Phys. Rev. B **46**, 14 201 (1992).
[26]J. B. Marston and C. Zeng, J. Appl. Phys. **69**, 5962 (1991).
[27]C. Chubrikov, Phys. Rev. Lett. **69**, 832 (1992).
[28]Y. R. Wang, Phys. Rev. B **45**, 12 604 (1992).
[29]H. J. Lauter, H. P. Schildberg, H. Godfrin, H. Wiechert, and R. Haensel, Can. J. Phys. **65**, 1435 (1987).
[30]D. S. Greywall and P. A. Busch, Phys. Rev. Lett. **62**, 1868 (1989).